

## Vapor–Liquid Equilibrium of Ammonia–Water–Lithium Nitrate Solutions

A. Sathyabhama<sup>1</sup> and T.P. Ashok Babu<sup>2</sup>

<sup>1</sup>Dept. of Mech. Eng. NITK, Surathkal / Faculty MSRIT, Vidya Soudha, MSR Nagar, MSRIT Post, Bangalore-560 054 Karnataka, India

<sup>2</sup>Dept. of Mech. Eng. NITK, Surathkal Post Srinivasnagar, Mangalore- 575 025 Karnataka, India

Experimental results on the pressure–temperature data for the NH<sub>3</sub>-H<sub>2</sub>O binary and NH<sub>3</sub>-H<sub>2</sub>O-LiNO<sub>3</sub> ternary solutions are reported. The pressure was varied between 100 and 800 kPa, while the mass fraction of ammonia was varied in the range 0–0.30. The lithium nitrate concentration of the solution was chosen in the range of 10–50% of mass ratio of lithium nitrate in pure water. An analytical equation for the equilibrium pressure as a function of temperature and concentration was obtained with a good fit to experimental data. © 2011 Wiley Periodicals, Inc. Heat Trans Asian Res, 40(6), 483–494, 2011; Published online 31 May 2011 in Wiley Online Library (wileyonlinelibrary.com/journal/htj). DOI 10.1002/htj.20351

**Key words:** vapor–liquid equilibrium, ternary mixture, NH<sub>3</sub>-H<sub>2</sub>O, NH<sub>3</sub>-LiNO<sub>3</sub>, NH<sub>3</sub>-H<sub>2</sub>O-LiNO<sub>3</sub>, correlation

### 1. Introduction

Absorption refrigeration systems have attracted increasing research interests in recent years. Unlike mechanical vapor compression refrigerators, these systems cause no ozone depletion and reduce demand on electricity supply. Besides, heat-powered systems could be superior to electricity-powered systems in that they harness inexpensive waste heat, solar, biomass, or geothermal energy sources for which the cost of supply is negligible in many cases. This makes heat-powered refrigeration a viable and economic option. The most common absorption systems are H<sub>2</sub>O-LiBr and NH<sub>3</sub>-H<sub>2</sub>O cycles. The advantage for refrigerant ammonia is that it can evaporate at lower temperatures compared to water. Therefore, for refrigeration, the NH<sub>3</sub>-H<sub>2</sub>O cycle is used. Research has been performed for NH<sub>3</sub>-H<sub>2</sub>O systems theoretically and experimentally. These studies show that the NH<sub>3</sub>-H<sub>2</sub>O system exhibits a relatively low COP. Also water as an absorbent has the limitation that stems from the appreciable vapor pressure of water. The ammonia vapor that is desorbed from the NH<sub>3</sub>-H<sub>2</sub>O mixture always includes a small fraction of water vapor.

The latter, if not removed by rectification, is detrimental, as water accumulates in the evaporator increasing the evaporator pressure. Efforts are being made to search for better refrigerant-absorbent pairs that can improve system performance. One of the alternate systems proposed is NH<sub>3</sub>-LiNO<sub>3</sub> but it has some drawbacks due to its high viscosity, inferior heat, and mass transfer characteristics and crystallization under some conditions. In order to keep the advantages and to

© 2011 Wiley Periodicals, Inc.

overcome the problems, the two  $\text{NH}_3\text{-H}_2\text{O}$  and  $\text{NH}_3\text{-LiNO}_3$  systems can be combined. Compared to the  $\text{NH}_3\text{-H}_2\text{O}$  system, the ternary mixture reduces the amount of water in the vapor phase, which means less or no rectification and compared to the  $\text{NH}_3\text{-LiNO}_3$  system, the ternary has a lower viscosity and avoids the crystallization problems.

The first to propose the  $\text{NH}_3\text{-H}_2\text{O-LiNO}_3$  ternary system was Davis et al. [1]. Reiner and Zaltash [2] also proposed this system but neither one presented enough data in order to characterize the system from the point of view of absorption cycles. Ehmke [3] presented the most important study of the properties of this system. The effects of the water content on the crystallization and viscosity were studied. Ehmke also determined and correlated the density and the vapor pressure of the system with water content of 25%. The vapor pressure of  $\text{NH}_3\text{-H}_2\text{O-LiNO}_3$  and  $\text{NH}_3\text{-LiNO}_3$  mixtures was measured by a static method from (293.15 to 353.15) K in ammonia mass fractions ranging from 0.2 to 0.6 by Libotean et al. [4].

The aim of the present paper is to obtain the pressure–temperature data for  $\text{NH}_3\text{-H}_2\text{O}$  and  $\text{NH}_3\text{-H}_2\text{O-LiNO}_3$  ternary systems at different mass fractions of ammonia and lithium nitrate.

## 2. Experimental Setup

The experimental setup used to measure the pressure–temperature data for  $\text{NH}_3\text{-H}_2\text{O}$  and  $\text{NH}_3\text{-H}_2\text{O-LiNO}_3$  mixtures is shown in Fig. 1. The unit consists of a boiling vessel, water pump, vacuum pump, condenser coil, and heater. The boiling vessel, 80 mm in diameter and 200 mm long, made of SS 316 is fitted with SS 316 flanges at the top and at the bottom as shown in Fig. 2. The vessel is fitted with two sight glasses to observe the equilibrium condition. The top flange has provisions for liquid charging, condenser cooling water inlet and outlet, vacuum pump, pressure transducer, and thermocouples to measure liquid and vapor temperatures. The bottom flange has provisions for heater and drain. A cylindrical alloy steel rod heater of diameter 6 mm and heating length 20 mm with an electrical heating element of 1 kW capacity mounted vertically within the boiling vessel is used to heat the solution to the saturation temperature.

## 3. Instrumentation

Two thermocouples (chrome alumel K type) are set, one in the liquid pool and other in the vapor region. These liquid and vapor temperatures confirm the system being maintained at the saturation state during the experiments. Thermocouples are calibrated at ice point. The uncertainty in the measurement of temperature is  $\pm 1$  K. The internal pressure of the boiling vessel is measured by a pressure transducer with an uncertainty of  $\pm 0.01$  bar. Pressure transducer is calibrated against a dead-weight balance. The power input to the heater is measured by an accurate digital power meter with  $\pm 1$  W uncertainty. The boiling vessel is well insulated. Electrical signals from the thermocouples, pressure transducer, and wattmeter are processed by a data acquisition system.

## 4. Experimentation

Before the start of each series of experiments, the boiling chamber was evacuated using a vacuum pump. The pressure of the boiling vessel was read on the logger display. Once the evacuation process was completed, the boiling vessel was filled with liquid solution. The test pressure was set in the logger. When the system was ready, the tests were started by giving a heat input to the rod heater.

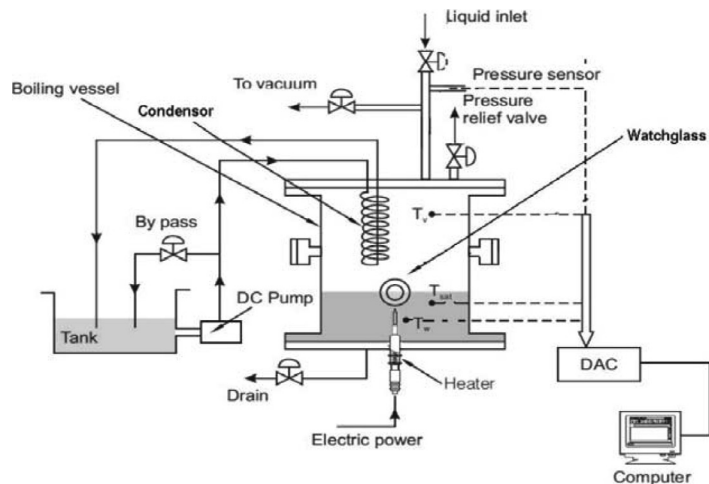


Fig. 1. Experimental setup.

The magnitude of the heat input was known from the wattmeter. The set pressure was maintained constant throughout an experiment by the combination of the cooling water pump, pressure transducer, and a proportional integral derivative (PID) pressure controller. The PID senses the pressure level in the boiling chamber through a pressure transducer and compares it with the set value fed to it by the researcher. To go from a higher pressure level to a lower pressure level, the PID sends a signal to the cooling water pump to open the suction line and pump water through the condenser coils. When the temperature and the pressure became stable, the data acquisition was started.

Commercially available aqueous ammonia solution of 99.99% purity supplied by Nice Chemicals was used in this study. Distilled water was used to dilute the aqueous ammonia. Concentration of the solution was measured by titration and the repeatability in the concentration measurement is  $\pm 0.3\%$ . Anhydrous lithium nitrate, assay 98% (supplied by John Baker Inc., Colorado, USA),



Fig. 2. Boiling vessel.

purity 98.999%, is used. Measurement of the weight of the salts was done using a weighing scale having a count of at least 0.1 gm. Ternary solution was prepared by mixing measured quantity of salts into the measured quantity of ammonia–water solution. The saturation temperature of each binary solution was measured over the pressure range: 100–800 kPa.

Subsequently, a measured quantity of LiNO<sub>3</sub>-H<sub>2</sub>O solution of known lithium nitrate concentration was added and the ternary mixture was heated to saturation temperature by giving heat input via the rod heater. After equilibrium was reached, the saturation temperature was noted down and the set pressure was changed. The measurements were performed in the pressure range  $p = 100$  to 800 kPa. The LiNO<sub>3</sub> concentration of the solution was chosen in the range of 10–50% of mass ratio of LiNO<sub>3</sub> in pure water.

## 5. Experimental Results

### 5.1 Performance validation

Distilled water was selected to verify the effectiveness of the experimental system. The calibration experiment was done before the binary and ternary mixture measurements with distilled water as the working fluid. The test pressure range was from ambient pressure to 800 kPa. The comparison between the experimental  $p$ - $T$  data and the data tabulated in ASHRAE Fundamentals [5] is presented in Fig. 3. The experimental data coincided well with the data given in the ASHRAE Fundamentals. The temperature deviation data is presented in Fig. 4. The average deviation is calculated as

$$Avg.Dev. = \frac{\sum \left| \frac{T_{exp} - T_{lit}}{T_{lit}} \right|}{n}, \quad n = \text{number of data points} \quad (1)$$

The average data deviation is 0.68%. This confirms the reliability and accuracy of the experimental setup.

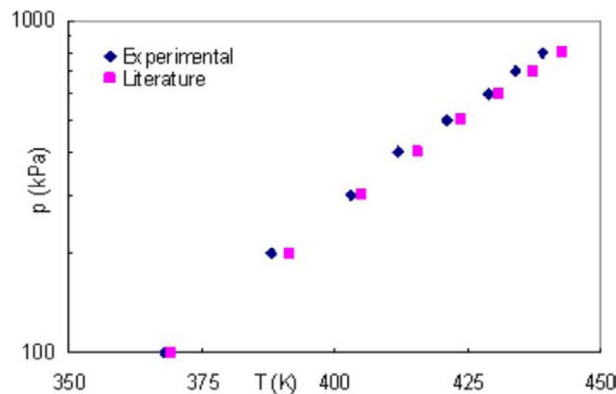


Fig. 3.  $p$ - $T$  data of distilled water. [Color figure can be viewed in the online issue, which is available at [wileyonlinelibrary.com/journal/htj](http://wileyonlinelibrary.com/journal/htj).]

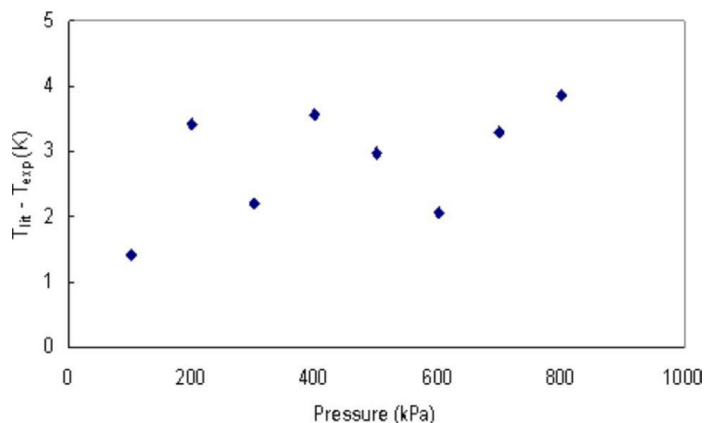


Fig. 4. Comparison between measured and literature temperature data.

## 5.2 $p$ - $T$ data of ammonia–water binary mixture

The mass fraction of ammonia is defined as follows:

$$x_{\text{NH}_3} = \frac{m_{\text{NH}_3}}{m_{\text{NH}_3} + m_{\text{H}_2\text{O}}} \quad (2)$$

The saturation temperature of the  $\text{NH}_3$ - $\text{H}_2\text{O}$  solution was measured from 100 kPa to 800 kPa, at 100 kPa intervals, for an ammonia mass fraction from 0 to 0.30. The saturation temperature increases with an increase in pressure at constant ammonia mass fraction and decreases with an increase in ammonia mass fraction at constant pressure.

### 5.2.1 Comparison with literature data

Although equilibrium data for a  $\text{NH}_3$ - $\text{H}_2\text{O}$  mixture have been reported in the literature, the conditions reported the experimental method, the concentration, and pressure ranges investigated are different from that of this study. An attempt was made to compare the experimental data obtained in this study with those reported by Smolen et al. [6]. There is good correspondence between this work and the data of Smolen et al. in the lower concentration range but the present data deviates slightly at higher concentrations as seen in Fig. 5. The experimental data are also compared with those predicted using the correlation of Patek and Klomfar [7] which overpredicts the present experimental data.

The experimental values of pressure,  $p$  (kPa), temperature,  $T$  (K), and liquid-phase mass fraction of ammonia ( $x_{\text{NH}_3}$ ) of the  $\text{NH}_3$ - $\text{H}_2\text{O}$  mixture were correlated using a polynomial equation similar to that proposed by Cacciola et al. [8].

$$\ln(p) = \sum_{i=0}^4 A_i x_{\text{NH}_3}^i + \frac{\sum_{i=0}^4 B_i x_{\text{NH}_3}^i}{T} \quad (3)$$

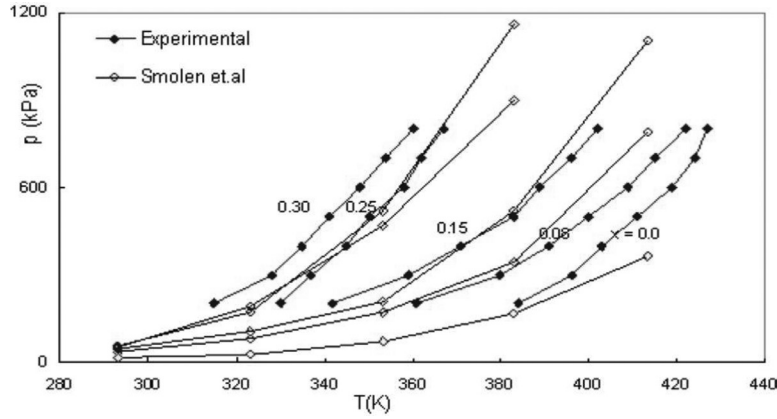


Fig. 5. Othmer diagram ( $p$ - $T$ - $x$ ) of mixture  $\text{NH}_3$ - $\text{H}_2\text{O}$  along with data of Smolen et al.

The values of the adjustable parameters  $A_i$  and  $B_i$  are shown in Table 1. Good agreement is achieved between the measured and calculated data using Eq. (3) as seen from Fig. 6. Figure 7 shows the deviation between experimental saturation temperature ( $T_{\text{exp}}$ ) and predicted saturation temperature ( $T_{\text{pre}}$ ). The average deviation between experimental saturation temperature ( $T_{\text{exp}}$ ) and predicted saturation temperature ( $T_{\text{pre}}$ ) data for the  $\text{NH}_3$ - $\text{H}_2\text{O}$  binary mixture is 0.0063.

### 5.3 $p$ - $T$ data of ammonia–water–lithium nitrate ternary mixture

The concentration of lithium nitrate is expressed as weight percentage on a salt-free solution basis as defined below [Eq. (4)]:

$$x_{\text{LiNO}_3} = \frac{m_{\text{LiNO}_3}}{m_{\text{LiNO}_3} + m_{\text{H}_2\text{O}}} \quad (4)$$

The saturation temperature of the  $\text{NH}_3$ - $\text{H}_2\text{O}$ - $\text{LiNO}_3$  solution was measured from 100 kPa to 800 kPa, at 100 kPa intervals, for an ammonia mass fraction from 0.15 to 0.30 and for the  $\text{LiNO}_3$  concentration from 0.10 to 0.50.  $p$ - $T$ - $x$  data for the ternary mixture were fitted to Eq. (5), where  $A_i$  and  $B_i$  are polynomial functions of the lithium nitrate mass fraction as shown in Eq. (6).

Table 1. Coefficients of Eq. (3) for the  $\text{NH}_3$ - $\text{H}_2\text{O}$  System

Coefficient	Value	Coefficient	Value
$A_0$	18.716	$B_0$	-5147.1
$A_1$	-26.776	$B_1$	14924.92
$A_2$	-668.732	$B_2$	210963
$A_3$	6363.629	$B_3$	-2153331
$A_4$	-13041.63	$B_4$	4473850

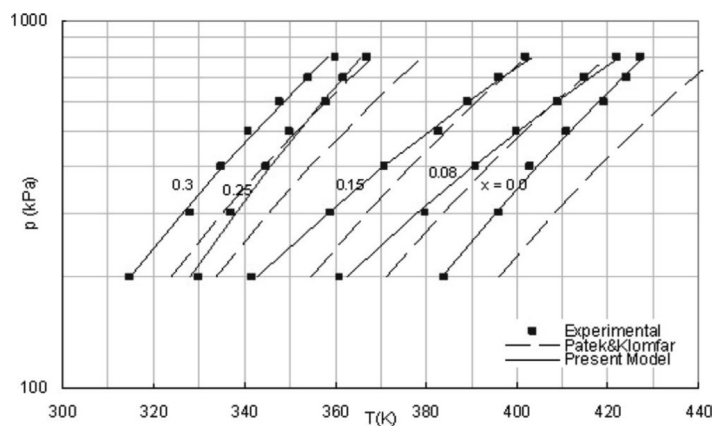


Fig. 6. Othmer diagram ( $p$ - $T$ - $x$ ) for mixture  $\text{NH}_3$ - $\text{H}_2\text{O}$  along with the values predicted from Patek and Klomfar correlation and Eq. (2).

$$\ln(p) = \sum_{i=0}^2 A_i x_{\text{NH}_3}^i + \frac{\sum_{i=0}^2 B_i x_{\text{NH}_3}^i}{T} \quad (5)$$

$$A_i = \sum_{j=0}^3 a_{ij} x_{\text{LiNO}_3}^j \quad B_i = \sum_{j=0}^3 b_{ij} x_{\text{LiNO}_3}^j \quad \text{for } i = 0, 1, 2 \quad (6)$$

The values of the adjustable parameters  $a_{ij}$  and  $b_{ij}$  are shown in Table 2. Good agreement is achieved between the measured and calculated data as seen from Figs. 8 and 9.

Table 3 shows the increase in bubble temperature of  $\text{NH}_3$ - $\text{H}_2\text{O}$  system with the addition of lithium nitrate at a different concentration of ammonia and lithium nitrate. The measurements are presented in Figs. 8 and 9. Each line in Fig. 8(a) represents the boiling point for one set of lithium

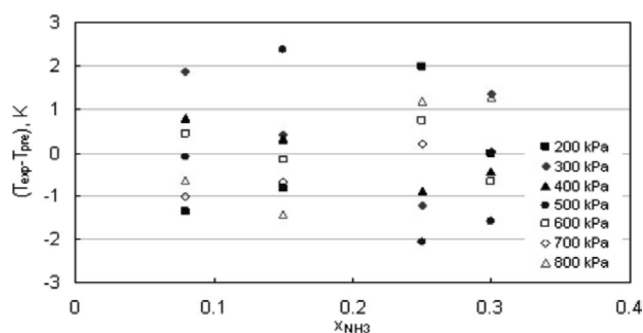


Fig. 7. Deviation between measured and predicted values of saturation temperature for the binary mixture  $\text{NH}_3$ - $\text{H}_2\text{O}$ .

Table 2. Coefficients of Eq. (5) for the NH<sub>3</sub>-H<sub>2</sub>O-LiNO<sub>3</sub> Systems

Coefficient	Value	Coefficient	Value
a <sub>00</sub>	-12.396	b <sub>00</sub>	5859.5
a <sub>01</sub>	54.448	b <sub>01</sub>	-31681
a <sub>02</sub>	-172.54	b <sub>02</sub>	133144
a <sub>03</sub>	287.6	b <sub>03</sub>	-199093
a <sub>10</sub>	262.07	b <sub>10</sub>	-88837
a <sub>11</sub>	-242.71	b <sub>11</sub>	180989
a <sub>12</sub>	157.47	b <sub>12</sub>	-637290
a <sub>13</sub>	-713.67	b <sub>13</sub>	1045933
a <sub>20</sub>	-550.53	b <sub>20</sub>	191187
a <sub>21</sub>	160.2	b <sub>21</sub>	-242171.3
a <sub>22</sub>	1607	b <sub>22</sub>	589040
a <sub>23</sub>	-1090	b <sub>23</sub>	-1207267

nitrate concentration for the solution with ammonia mass concentration of 30%. As can be seen from Fig. 8(a), an increase in lithium nitrate concentration increases the boiling point of the solution for constant ammonia concentration in the solution. Similar trends are obtained for 25% and 15% ammonia concentration solutions as depicted in Figs. 8(b) and (c), respectively.

An increase in ammonia concentration decreases the boiling point, as can be seen from Figs. 9(a)–(c). In Figs. 8 and 9, the lines represent the saturation temperature predicted using Eq. (4). The deviation between experimental data and that predicted using Eq. (4) is shown in Fig. 10. The effect of lithium nitrate concentration and ammonia concentration on the boiling point at different pressures is shown in Fig. 11. The saturation temperature increases with an increase in both pressure and lithium

Table 3. Saturation Temperature of the NH<sub>3</sub>-H<sub>2</sub>O and NH<sub>3</sub>-H<sub>2</sub>O-LiNO<sub>3</sub> Systems

Pressure (kPa)	Saturation Temperature (K)											
	x <sub>NH<sub>3</sub></sub> =0.30				x <sub>NH<sub>3</sub></sub> =0.25				x <sub>NH<sub>3</sub></sub> =0.15			
	x <sub>LiNO<sub>3</sub></sub> =0.00	x <sub>LiNO<sub>3</sub></sub> =0.10	x <sub>LiNO<sub>3</sub></sub> =0.30	x <sub>LiNO<sub>3</sub></sub> =0.50	x <sub>LiNO<sub>3</sub></sub> =0.00	x <sub>LiNO<sub>3</sub></sub> =0.10	x <sub>LiNO<sub>3</sub></sub> =0.30	x <sub>LiNO<sub>3</sub></sub> =0.50	x <sub>LiNO<sub>3</sub></sub> =0.00	x <sub>LiNO<sub>3</sub></sub> =0.10	x <sub>LiNO<sub>3</sub></sub> =0.30	x <sub>LiNO<sub>3</sub></sub> =0.50
100					313	316	320	323	320	334		
200	315				330	330	335	338	342	358	353	363
300	328				337	339	345	350	359	373	368	376
400	335	339	343	352	345	347	354	359	371	383	383	387
500	341				350	354	361	365	383	393	390	395
600	348	353	357	364	358	360	367	375	389	399	399	402
700	354				362	365	373	379	396	405	404	408
800	360	363	367	377	367	370	379	383	402	411	411	413



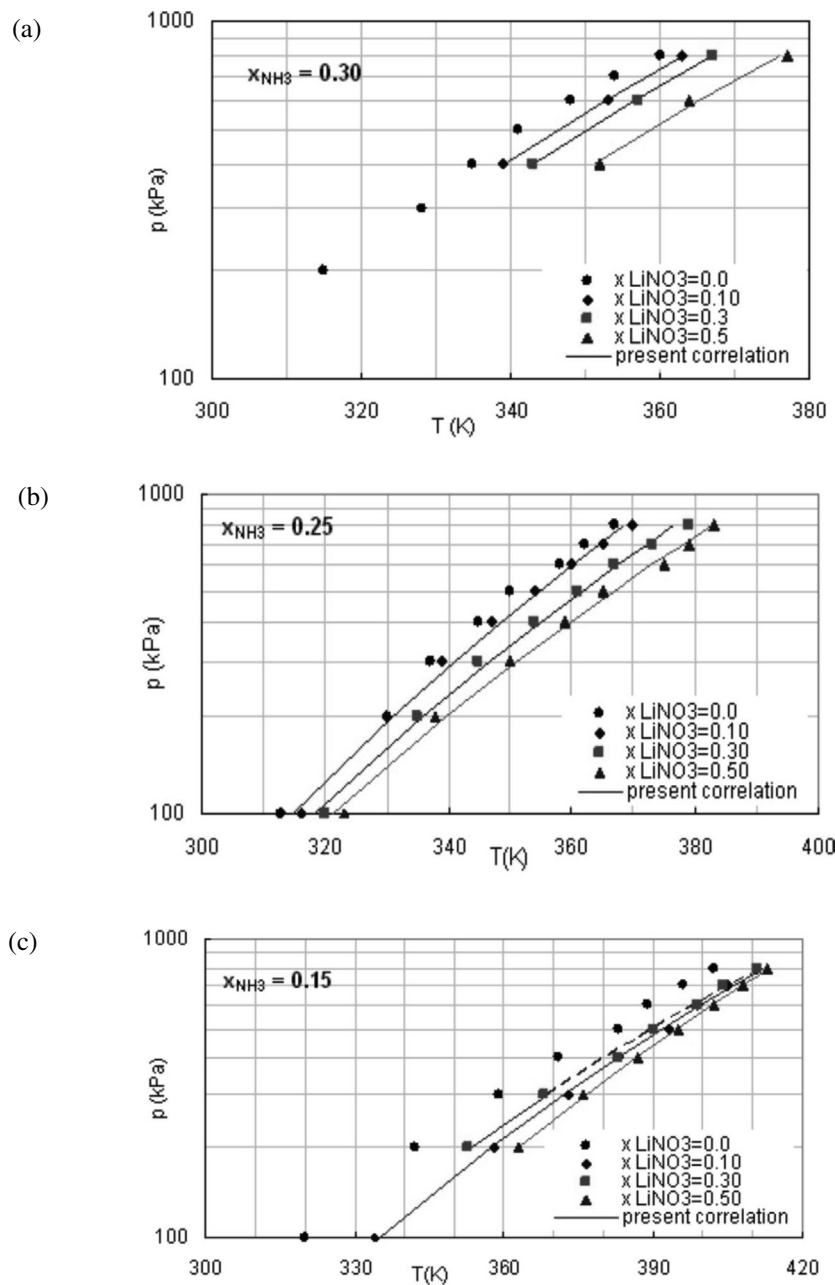


Fig. 8. Saturation temperature for different concentrations of ammonia.

nitrate concentration. The average deviation between experimental saturation temperature ( $T_{\text{exp}}$ ) and predicted saturation temperature ( $T_{\text{pre}}$ ) data for the  $\text{NH}_3\text{-H}_2\text{O-LiNO}_3$  ternary mixture was 0.0375.

In Fig. 12, the behavior of the saturation temperature as a function of the ammonia mass concentration and lithium nitrate mass concentration, at a pressure of 400 kPa, is shown in a three-dimensional plot.

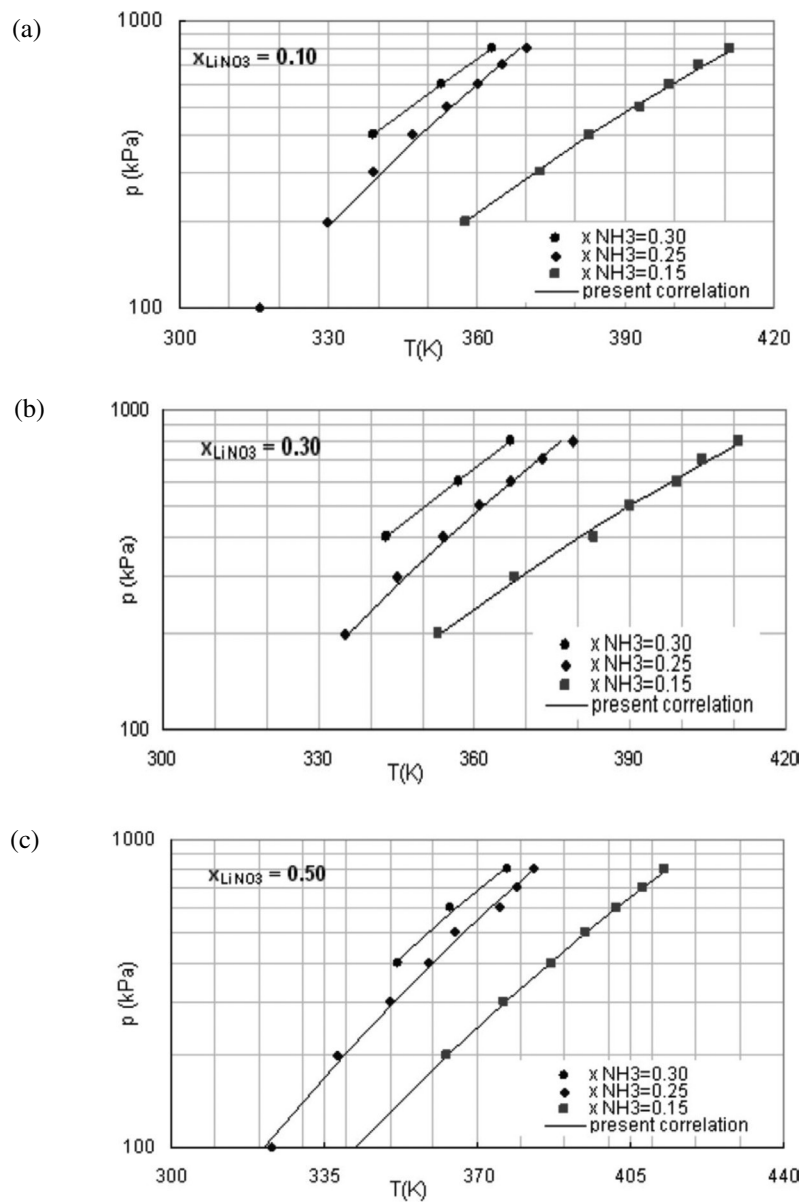


Fig. 9. Saturation temperature for different concentrations of lithium nitrate.

## 6. Conclusion

The  $p$ - $T$  data of the  $NH_3$ - $H_2O$ - $LiNO_3$  ternary mixture was measured in the pressure range of 100–800 kPa by varying the mass fraction of ammonia from 0.15–0.30. The lithium nitrate concentration of the solution was chosen in the range of 10–50% of mass ratio of lithium nitrate in pure water. The saturation temperature of the  $NH_3$ - $H_2O$  mixture increases with the addition of lithium nitrate. In addition, the saturation temperature of the  $NH_3$ - $H_2O$  binary mixture was determined from 100 kPa to 800 kPa for an ammonia total mass fraction from 0.15 to 0.30. Vapor pressure, temperature,

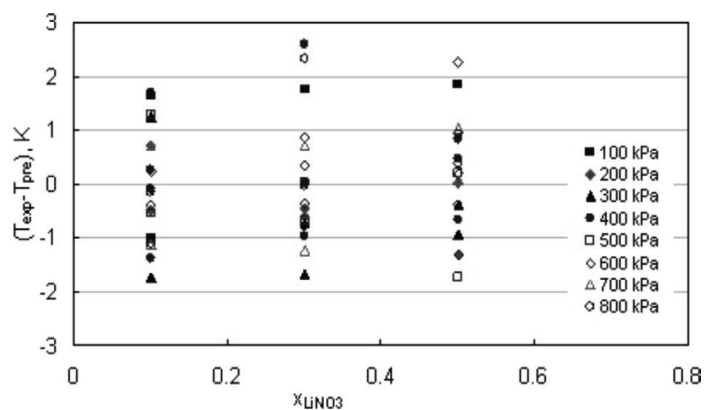


Fig. 10. Deviation between measured and predicted values of saturation temperature for the  $\text{NH}_3\text{-H}_2\text{O-LiNO}_3$  ternary mixture.

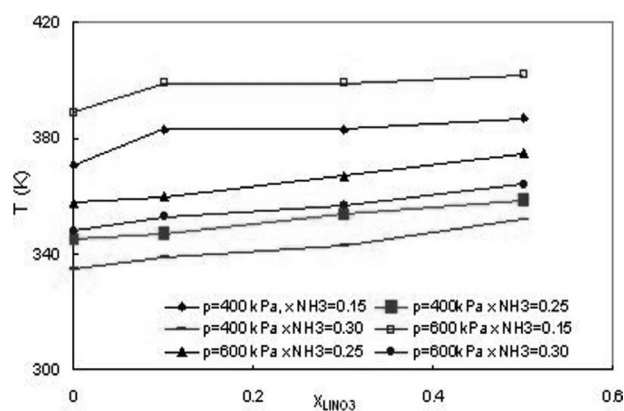


Fig. 11. Effect of ammonia and lithium nitrate concentration on saturation temperature.

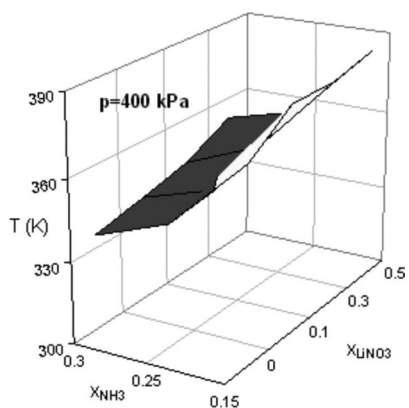


Fig. 12. Saturation temperature as a function of ammonia and lithium nitrate concentration.

and liquid-phase composition were correlated using an empirical equation. Calculated and measured data showed good agreement. The average deviation between experimental saturation temperature ( $T_{\text{exp}}$ ) and predicted saturation temperature ( $T_{\text{pre}}$ ) data for the  $\text{NH}_3\text{-H}_2\text{O}$  binary mixture was 0.0063 and that for the  $\text{NH}_3\text{-H}_2\text{O-LiNO}_3$  ternary mixture was 0.0375.

#### Literature Cited

1. Davis ROE, Olmstead LB, Lundstrum FO. Vapor pressure of ammonia-salt solutions. *J Am Chem Soc* 1921;43:1580–1583.
2. Reiner RH, Zaltash A. Densities and viscosities of ternary ammonia/water fluids. ASME Winter Annual Meeting, New Orleans, Nov. 28–Dec. 3, 1993.
3. Ehmke HJ. Doctoral thesis. University Essen, Essen, Germany, 1984.
4. Libotean S, Salavera D, Valles M, Esteve X, Coronas A. Vapor-liquid equilibrium of ammonia + lithium nitrate + water and ammonia + lithium nitrate solutions from (293.15 to 353.15) K. *J Chem Eng Data* 2007;52:1050–1055.
5. ASHRAE Fundamentals (2005), Thermophysical properties of refrigerants, 34–35.
6. Smolen MT, David BM, Bruce CP. Vapour-liquid equilibrium data for the  $\text{NH}_3\text{+H}_2\text{O}$  system and its description with a modified cubic equation of state. *J Chem Eng Data* 1991;36:202–208.
7. Patek J, Klomfar J. Simple functions for fast calculations of selected thermodynamic properties of the ammonia-water system, *Int J Refrig* 1995;18:228–234.
8. Cacciola G, Restuccia G, Aristov Y. Vapour pressure of (potassium hydroxide + ammonia + water) solutions. *J Chem Eng Data* 1995;40:267–270.

